UNIVERSITY OF ILLINOIS URBANA-CHAMPAIGN

Prairie Research Institute
Illinois State Geological Survey
615 E. Peabody Drive, MC-650
Champaign, IL 61820-6918

June 25, 2024

Luminescence dating report for Dr. Andrew Sadowski, from the Washington Geological Survey

ISGS code	Sample	Grain Size (µm)	Equivalent dose (Gy) [1]	Dose rate (Gy/ka)	Age (ka) [1]	n (accepted/total)
953	Ess167	150 - 250	8.3 ± 0.5	2.79 ± 0.10	3.0 ± 0.2	9/9
954	Ess224	90 - 150	14.6 ± 1.8	2.52 ± 0.10	5.8 ± 0.8	9/9
955	Ess225	90 - 150	15.2 ± 1.3	2.56 ± 0.11	5.9 ± 0.6	9/9

[1] fading corrected (Huntley and Lamothe, 2001)

Optically stimulated luminescence (OSL) dating was measured on K-feldspar, on small aliquots. The age was corrected for anomalous fading, by following an individual aliquot approach. Uncertainties are reported at a 1σ significance, providing a level of confidence of approximately 67%. The uncertainties combine random and systematic errors, added in quadrature. The beta dose rate on the luminescence system was calibrated against the Risø quartz calibration batch 90, and updated to the latest value (Autzen et al., 2022). Further details can be found in the report.

Sebastien Huot, Ph.D.

Illinois State Geological Survey

Champaign, Illinois

shuot@illinois.edu

+1-217-300-2579 (office)

This is a report on the optically stimulated luminescence (IRSL) dating of a single sample delivered to us by Dr. Andrew Sadowski, during Summer 2023. Thes samples were retrieved in an opaque tube, from outcrops. The depositional environment is interpreted as loess (Ess167) or alluvial fan (Ess224, Ess225). The alluvial fan is expected to be old, very old (100 – 500 ka). For the purposes of internal identification, we labeled this sample ISGS 953-955.

1. Sample preparation and equipment

The tubes were opened and the mineral extraction was conducted in a subdued orange light environment. One inch of sediment (i.e. the external portion) was removed from both ends of each tube because these might have been partially exposed to light during sampling. Sediment from the external portions was used to measure the in situ water content and its radioactive content (uranium, thorium, and potassium), both for dose rate calculation. These minerals were wet sieved to retrieve the 90- to 250-µm grain size. A hydrochloric acid attack (HCl, 10%) was applied to dissolve any carbonate minerals that might be present. Using a heavy liquid solution (2.58 g/mL) of lithium heteropolytungstate (LST), we separated K-feldspar (<2.58) from the quartz and Na-feldspar minerals (>2.58). There was an unusually large amount of low density minerals. The initial luminescence signal observed from these K-feldspar minerals were unusually dim. To further increase the purity of these K-feldspar, we made use of a Frantz magnetic separator and relied on the non-magnetic fraction (0.7 ampere) for IRSL dating. A lot of minerals had a paramagnetic property. Personal experience has shown me that these paramagnetic minerals, contaminating the K-feldspar low density fraction do not emit any luminescence signal. These purified K-feldspar grains displayed a bright luminescence signal, as is typical.

The beta dose rate on the luminescence system was calibrated against the Risø quartz calibration batch 90, and was updated to the latest value (Autzen et al., 2022). Please note that Risø has refined the calculated value, attributed to their quartz calibration, by further constraining the systematic uncertainties, inherent to that process. This results in a calculated OSL/IRSL age increase by 8.25 %. This retrospectively affects all luminescence ages, measured since the year 2000, from every luminescence dating laboratories around the world that relies on the Risø quartz calibration (batch 1 through 125).

To obtain the dose rate, sediments from the external portion of each sampling tube were dried, then ash (500°C, 24 hours), and a representative portion was encapsulated in thin disk-shaped containers (~20 g) and sealed with 2 layers of epoxy gel. A minimum waiting time of 21 days after sealing is recommended to restore the radioactive equilibrium of radon-222 daughter products (Gilmore, 2008). The specific activities (Bq/kg) were measured with a broad-energy high-purity germanium detector (BEGe), in a planar configuration, shielded by 15 cm of lead. Efficiency calibration of the detector was obtained with a set of six certified standards (IAEA-RGU-1, IAEA-RGTh-1, IAEA-RGK-1, IAEA-385, NIST 4350b, and NIST 4355).

2. Equivalent dose (De) measurements

For the equivalent doses (De) measurements, we relied on an automated Risø TL-DA-20 system, equipped with a set of blue (470 nm) and infrared (870 nm) LEDs, for light stimulation. Detection was made in the blue (combination of Schott BG39 and Corning 7-59 glass filters) for K-feldspar. For each sample, we dispensed K-feldspar grains over a small area (2 mm), onto a silicon oil covered stainless disk (10 mm diameter). Around 20 - 50 grains were dispensed on each disks' center. Several aliquots were measured, for each sample.

IRSL measurements were carried out with a single-aliquot regenerative dose (SAR) protocol (Table 1). The optimal measurement parameters were selected by a dose recovery test (latent dose bleached with sunlight for 1 day). An initial dose was given at first (that was a close match to the measured equivalent dose for each sample; 250 Gy) and it was subsequently recovered by measuring its equivalent dose with the SAR protocol. The samples responded reasonably well to the treatment. From this we selected a preheat temperature (Lx and Tx) of 250°C (held for 60 seconds; Huot and Lamothe, 2003). The dose recovery test was performed for every sample using the most appropriate temperature. It yielded an average measured-to-given dose ratio of 0.97 ± 0.03. This outcome is positive. Considering this result, we opted to select the parameters in Table 1.

Table 1. Measurement steps for the single-aliquot regenerative protocol (Huot and Lamothe, 2003; Murray and Wintle, 2000)

Step	Procedure (K-feldspar)
1	Regeneration[1]/natural dose
2	Preheat (250°C), hold for 60 seconds
3	Pause[2]
4	IRSL stimulation with IR LEDs at 50°C for 100 seconds (L_x)
5	Test dose beta irradiation (22 Gy)
6	Preheat (250°C) for 60 seconds
7	IRSL stimulation with IR LEDs at 50°C for 100 seconds (T_x)
8	Repeat Steps 1–7 with further regeneration doses

[1] For equivalent dose measurements, we gave a range of laboratory-induced doses that would properly encompass the variability of the observed natural luminescence.

[2] There was no pause for equivalent dose measurements. A pause was observed here for anomalous fading measurements.

2.1 Equivalent dose calculation

For the equivalent dose, all calculations were made using the "late light" approach for background subtractions, by taking the initial 5 data channels (5 seconds) from the IRSL decay curve and removing the background from the end of the stimulation curve (30 data channels, 30 seconds; Figure 1).

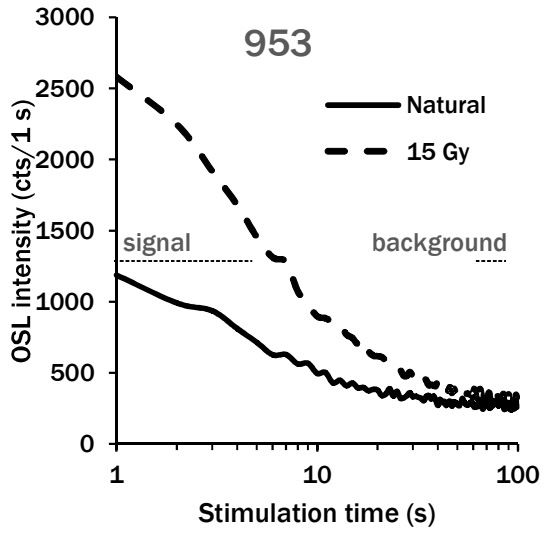

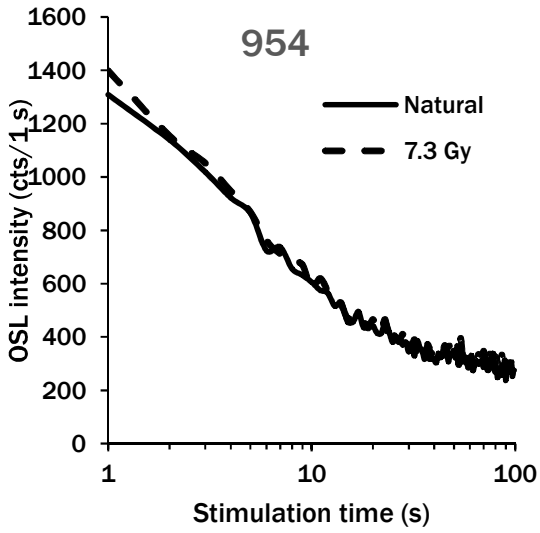

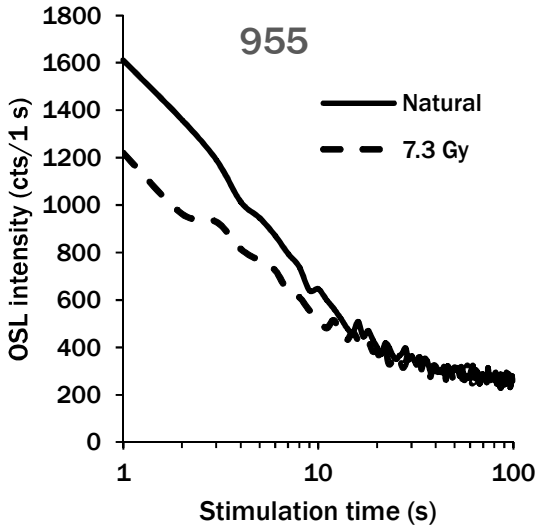

Figure 1. Typically IRSL decay curve, for a naturally dose aliquot (solid curve) or laboratory-induced dose (dashed curve, in Gy). The area under the curve is proportional to the dose of radiation stored within the mineral. Their luminescence growth curve and fading rate are shown in Figure 2 and 3. Note the logarithmic time axis.

Uncertainties relied on Poisson statistics. For curve fitting, we also propagated the uncertainties from the optimized luminescence growth curve parameters. In addition, when the observed scatter about the best fit regression line was too high, the uncertainties were increased (Figure 2). For this, we relied on the one-tailed probability χ^2 distribution, with N - 3 degrees of freedom (where N is the number of measured data points). When the probability was lower than 15% (i.e., the data points scattered above and beyond the best fit line), the uncertainties for the optimized parameters were expanded by Student's t values for N - 3 degrees of freedom (Brooks et al., 1972; Ludwig, 2003).

2.2. Anomalous fading

The luminescence of feldspar is known to underestimate the 'true' burial age, typically by about 30 to 50 % (Aitken, 1998). The cause is known to us: anomalous fading (Wintle, 1973). Luminescence dating is akin to a filling a glass with water. At time zero, the glass is empty (i.e. the zeroing effect of sunlight). You pour water into it, at a constant rate (dose rate), but stop before reaching the top (sampling). The volume of water contained in the glass represents the equivalent dose in luminescence (the total amount of radiation energy trapped by the mineral during burial). By dividing the volume (equivalent dose) by the rating of water filling (dose rate), we can calculate when was the glass empty (length of burial).

Now, what if there is a very small hole in the glass. As you pour water into it, you lose water through that hole, at a steady rate. Now, the volume of water that remains in the glass underestimates the real amount of water that was poured in it. If you can measure the size of the hole, it is possible to calculate what would have been the real amount of water contained in the glass.

The luminescence of quartz (our workhorse in luminescence dating) is akin to a perfect glass, whereas K-feldspar is that of a glass with a hole. At the time this phenomenon was first described in feldspar, the mechanism underlying that lost, or fading, was unknown to us; hence, it was termed 'anomalous fading'. It was 'anomalous' because from thermodynamic principles, it is expected that a trapped electron would remain so for many millions of years (i.e. water can evaporate from your glass) at room temperature (i.e. just like water, where the evaporation rate is temperature dependent, so is the thermal lifetime of a trapped electron). Yet, trapped elections in feldspar are leaking faster than they should and that rate of leakage is independent of temperature. Hence, anomalous!

Nowadays, we know how to deal with it. We know how to measure the size of the hole (fading rate; Auclair et al., 2003) and we know how to properly correct for it (e.g. Huntley and Lamothe, 2001). We acknowledge that a novel measurement technique to minimize, and sometimes circumvent, the IRSL age underestimation from anomalous fading has emerged in the literature (post-IR IRSL; Buylaert et al., 2012). An attempt was made for this sample; unfortunately, it yielded a very low

luminescence intensity. Therefore, we opted to retain the < old school > method (i.e. IRSL 50°C) of measuring and correcting for fading.

2.3 Fading corrected age

Measured IRSL ages were corrected for anomalous fading using the Huntley and Lamothe (2001). The fading rate was measured for each equivalent dose, aliquot by aliquot. After the equivalent dose measurement, the aliquots were bleached under normal sunlight, for one day. After, the anomalous fading measurement was initiated, using the same measurement parameters (Table 1). Thus, pairing equivalent dose with anomalous fading rate, aliquot by aliquot. The laboratory-induced dose (step 1) was fixed, at 58 Gy, along with a test dose (step 5) of 29 Gy. Also, there was a 'pause' in effect, at step 3, which ranged from 20 minutes up to 3 days (Figure 3; Auclair et al., 2003).

The < as measured > equivalent dose from each aliquot was corrected with the aid of the Huntley and Lamothe (2001) model. This has a limitation: it is accurate, as long as the equivalent dose is within the linear approximation of the luminescence growth curve. For these samples, the luminescence growth curve can be approximated to a simple straight line for radiation doses easily up to 200 Gy, and more (Figure 2). This is well above the measured equivalent doses for these samples. Over the years, this model has proven to be highly successful in yielding accurate ages, whenever an independent assessment could be made. We do acknowledge that a novel technique, termed pIRSL-IRSL, that promises to minimize, and perhaps truly circumvent the problem of anomalous fading, has gained a lot of popularity (Buylaert et al., 2012). We did test the water, with these samples. Unfortunately, the luminescence signal to noise ratio was too low; not surprisingly, as these samples are rather young.

2.4 Quartz measurements

Initially, the sample preparation for these samples focused exclusively on K-feldspar minerals, as these samples were expected to be old, very old. However, the initial age estimates indicated these samples were in fact young, much younger. Due to this, we went back to the dark laboratory, in order to extract quartz minerals. Sadly, the initial luminescence measurements on quartz minerals showed these samples were very dim. It was not a surprised, as quartz minerals around the Washington State, has a history of being unstable, yielding uncharacteristically low luminescence intensities (see their Figure 5; Mahan et al., 2023). At least, we gave it a try.

2.5 Age distribution

A weighted average (using the central age model; Galbraith et al., 1999) was used in all calculations, except when noted otherwise. The central age model provides an overdispersion parameter. This parameter characterizes the degree to which the observed weighted distribution is consistent with the predicted weighted distribution from the observed data. At 0%, the observed distribution is equal to the statistical prediction. In luminescence dating, it is common for the observed distribution to be slightly larger than the expected distribution by a value of approximately

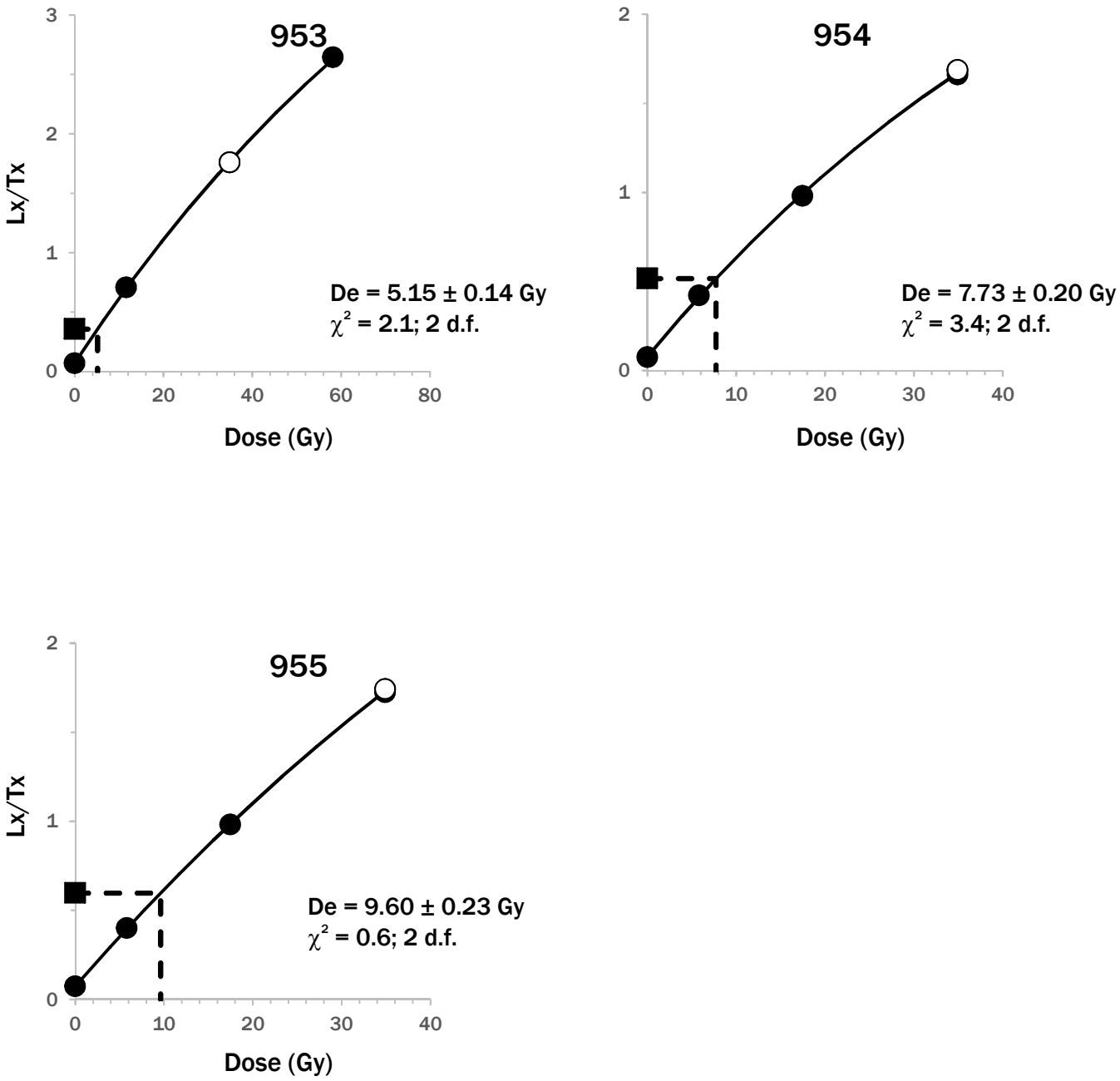

Figure 2. Luminescence dose response curve for the same aliquots shown in Figure 1. Each point corresponds to the OSL (Lx; measurement step 3 in Table 1) of a natural (square) or laboratory-induced dose (filled circles)), normalized by the luminescence response to a fixed test dose (Tx; measurement step 6). A repeat measurement (the recycling test; open circles) was performed at the end. The equivalent dose is obtained by interpolation. For the aliquots shown here, the observed measurements scatter well around the predicted best-fit curve.

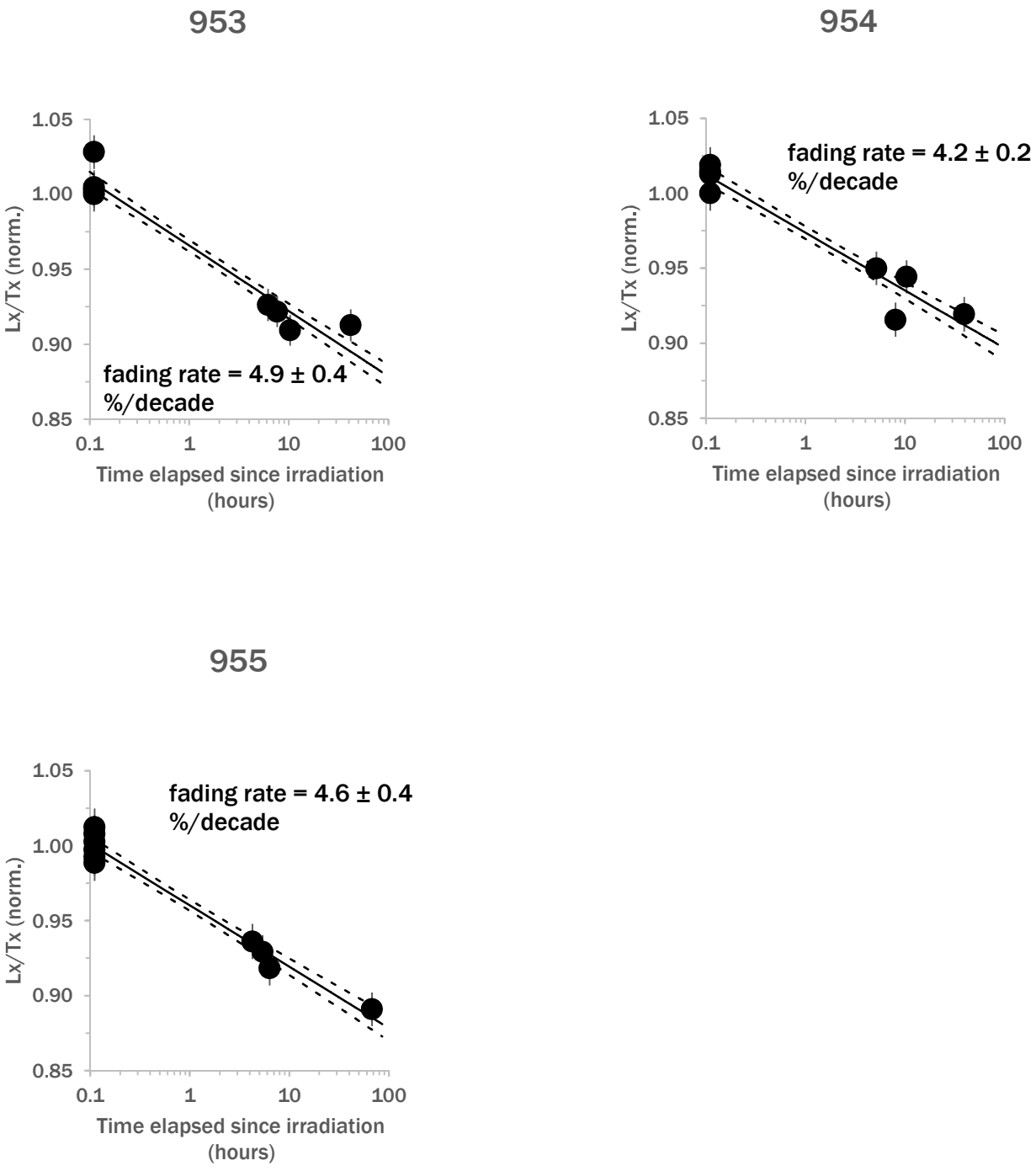

Figure 3. Anomalous fading measurement, for a representative aliquot of each sample (the same shown in Figure 1 and 2). Repeated measurement cycles are made, on the same aliquot, with different delays between the irradiation and the IRSL measurement (i.e. step 3 from Table 1). The slope is proportional to the fading rate, used in the fading correction model. The 2 dashed lines represent the 1σ error envelops. Note the logarithmic time axis.

20%. This means that the calculated uncertainties tend to underestimate the "real" uncertainties because of intrinsic (e.g., instrumental uncertainties, luminescence characteristics of quartz and K-feldspar) or extrinsic (e.g., partial bleaching, external beta microdosimetry) factors. The central age model expands the age uncertainty in an attempt to account for this discrepancy. Here, the overdispersion is within the normality (Table 2, Figure 4). The fading corrected age is presented in Table 3.

Table 2. Age overdispersion parameters[1]

ISGS code	Sample	Overdispersion (%)
953	Ess167	15 ± 5
954	Ess224	37 ± 9
955	Ess225	24 ± 7

[1]A value of 20% is typical in luminescence

Table 3. Measured versus corrected ages

		as measured			
ISGS code	sample	equivalent dose (Gy)	age (ka)	fading corrected age (ka)	average fading rate (%/decade)
953	Ess167	5.2 ± 0.3	1.88 ± 0.14	2.97 ± 0.23	5.18 ± 0.33
954	Ess224	9.7 ± 1.1	3.84 ± 0.49	5.80 ± 0.78	4.55 ± 0.35
955	Ess225	10.2 ± 0.7	3.99 ± 0.33	5.94 ± 0.59	4.43 ± 0.22

3. Dose rate

The water content was measured for each sample. The as-received water content was relatively moist (Table 4). It seems reasonable, given the fieldnotes provided to us (thank you!), along with the location of these deposits. We expect this state would have held, for most of the sediments' burial history. Given this, we opted for the values presented in the table. We assigned a water content uncertainty of 5 % to account for possible variation during the entire length of burial. The bulk density was assumed to be 1.6 g/cm3.

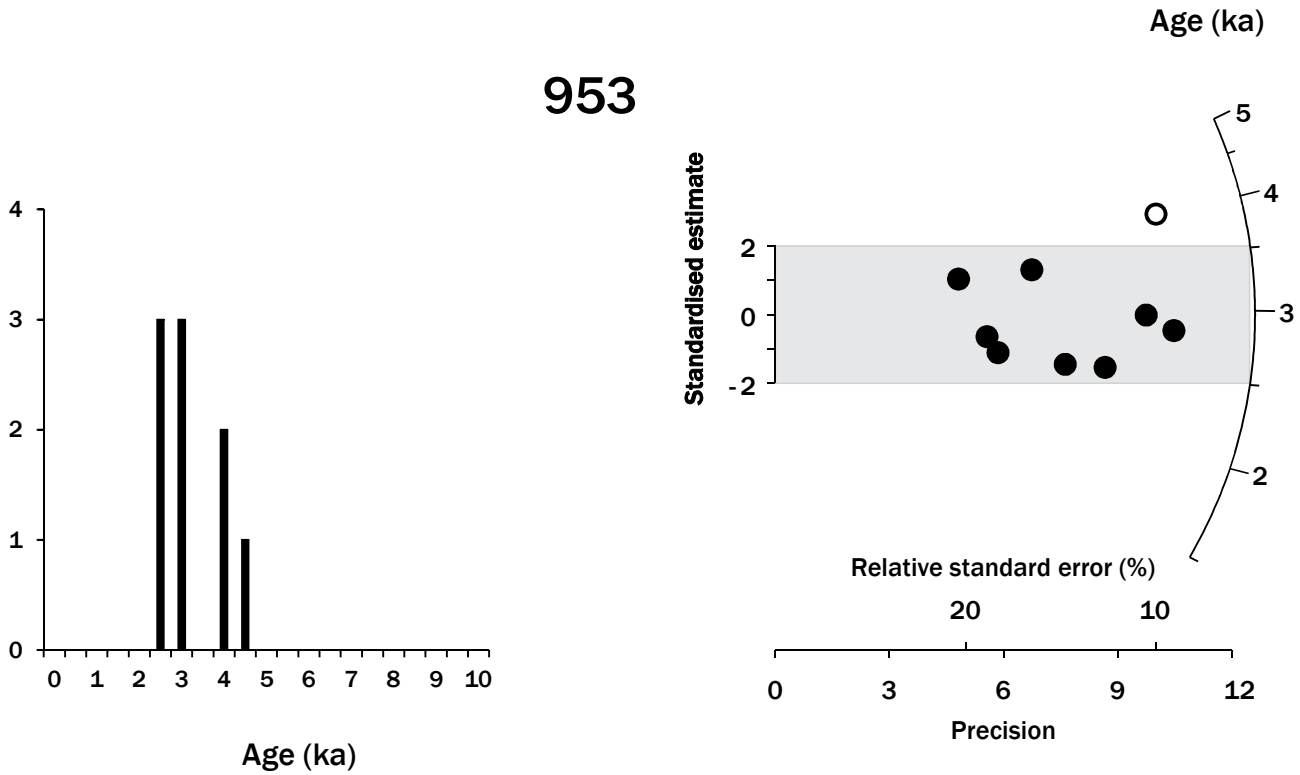

Figure 4a. Age distributions, as a histogram and a radial plot, for all samples. Each circle on the radial plot represents the age and uncertainty, for a single aliquot. The age is read on the arc axis, by drawing a straight line from (0, 0), passing through a circle and intersecting the radial axis (log scale). The (0, 0) coordinate corresponds to a 0 standardised estimate (y-axis) and 0 precision (x-axis). The uncertainty is read on the horizontal axis, by drawing a perpendicular line reaching a circle. Hence, two aliquots, having the same age, but with different uncertainty, will lay on the same straight line (from (0, 0) to the radial axis). The aliquot with the smaller uncertainty (higher precision) will be closer to the arc. Values (filled circles) within the light grey shaded band are consistent (at 2σ) with the weighted mean (Central Age Model). A cluster of aliquots within this shaded band expresses confidence that we have a population of grains consistent with a single age.

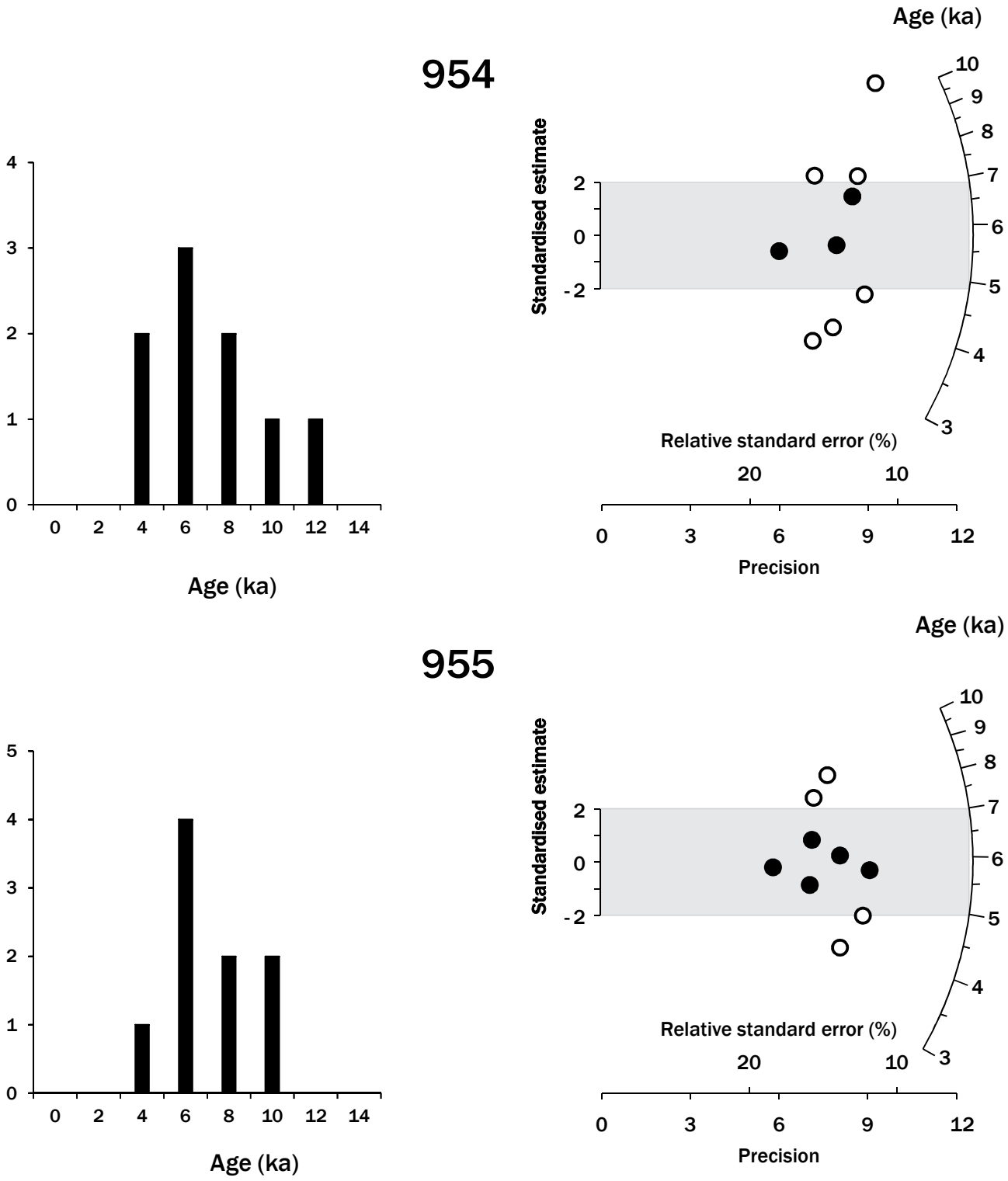

Figure 4b. Age distributions, as a histogram and a radial plot, for all samples. Each circle on the radial plot represents the age and uncertainty, for a single aliquot. The age is read on the arc axis, by drawing a straight line from (0, 0), passing through a circle and intersecting the radial axis (log scale). The (0, 0) coordinate corresponds to a 0 standardised estimate (y-axis) and 0 precision (x-axis). The uncertainty is read on the horizontal axis, by drawing a perpendicular line reaching a circle. Hence, two aliquots, having the same age, but with different uncertainty, will lay on the same straight line (from (0, 0) to the radial axis). The aliquot with the smaller uncertainty (higher precision) will be closer to the arc. Values (filled circles) within the light grey shaded band are consistent (at 2σ) with the weighted mean (Central Age Model). A cluster of aliquots within this shaded band expresses confidence that we have a population of grains consistent with a single age.

Table 4. Water content, measured from the sample, with the value presumed to have prevailed during the burial.

ISGS code	Sample	in situ (%)	presumed (%)
953	Ess167	7	10 ± 5
954	Ess224	9	10 ± 5
955	Ess225	11	10 ± 5

Waiting times of around 30 days were observed before measuring the radioactive activities of uranium, thorium, and potassium, from which we can derive contributions from alpha, beta, and gamma energy decay (Table 5).

Table 5. Specific activity (Bq/kg)

ISGS code	Sample	238U	226Ra	210Pb	232Th	40K	137Cs
953	Ess167	27.8 ± 1.7	25.2 ± 0.4	18.0 ± 1.8	26.8 ± 0.4	293.3 ± 8.0	N/A
954	Ess224	18.6 ± 1.3	22.7 ± 0.4	17.9 ± 1.4	23.6 ± 0.3	348.1 ± 7.0	0.6 ± 0.2
955	Ess225	22.3 ± 1.9	20.7 ± 0.4	19.0 ± 1.7	24.6 ± 0.4	342.9 ± 8.4	4.0 ± 0.3

For K-feldspar, we assumed an internal content of 12.5 ± 0.5 % and 400 ± 100 ppm, for potassium and rubidium, respectively (Huntley and Baril, 1997; Huntley and Hancock, 2001). A conservative 0.10 ± 0.05 “a value” (efficiency of alpha particles compared with beta particles upon inducing a trapped charge in quartz and feldspar; i.e., alpha is only 10% as effective as beta) was retained (Table 6).

It should be noted that all 3 samples had an organic smell, even though no visible organic matter was present. The loss to ignition ratio (ash, 500°C, 24 hours) was 5 – 6 %, for each. This greatly deviates from the typical OSL sample. This value is significant, and will skew the effective < dose rate >. For the moment, it was not taken into proper account. The values uranium, thorium, and potassium values (Table 5) are reliable, because each sample was ash. But an additional conversion factor must be introduced, to convert uranium, thorium, and potassium to dose rate values. If the need warrants it, please reach out to us.

Furthermore, 137Cs was positively detected, in both Ess224 and Ess225. This radioisotope is manmade, and appeared first in the environment in the early 1960s, following the early development of atomic bombs, detonated in the atmosphere. Therefore, 137Cs cannot be found in older sediment. Post-sedimentary processes, such as bioturbation or percolation, might entrain small particles deeper below the surface, where 137Cs adheres to the surface of particles. The smaller the grain sizes, the higher the surface area, thus, the higher the abundance of 137Cs per unit of mass.

Table 6. Contribution to the dose rate, expressed in Gy/ka

ISGS code	alpha external (Gy/ka)	beta internal (Gy/ka)	beta external (Gy/ka)	gamma (Gy/ka)	cosmic ray (Gy/ka)	depth (m)	water (%)	total (Gy/ka)
953	0.08 ± 0.05	0.81 ± 0.04	0.97 ± 0.07	0.70 ± 0.02	0.24 ± 0.01	0.62	10 ± 5	2.79 ± 0.10
954	0.10 ± 0.06	0.50 ± 0.03	1.06 ± 0.07	0.68 ± 0.02	0.19 ± 0.01	1.8	10 ± 5	2.52 ± 0.10
955	0.11 ± 0.07	0.50 ± 0.03	1.06 ± 0.08	0.67 ± 0.02	0.22 ± 0.01	0.66	10 ± 5	2.56 ± 0.11

.

4. Interpretation

The observed age scatter for sample Ess167 is noticeably lower than Ess224, Ess225. This might be attributed to the difference in depositional environment: loess (Ess167) versus alluvial fan (Ess224, Ess225). Everything else being equal, we can expect a comparable age scatter across similar samples. Hence, the (slightly) higher scatter for the alluvial fan samples might be an indication of < partial bleaching >.

Partial bleaching is a concept where, at time zero, at the end of the last sedimentary cycle (erosion, transport, deposition), only a fraction of quartz/K-feldspar minerals were sufficiently exposed to sunlight. It is an essential requirement for luminescence dating: at time zero, the age is zero, as long as the quartz/K-feldspar minerals were sufficiently exposed to sunlight. Otherwise, these insufficiently exposed minerals carry a residual age. Hence, in an age distribution, we expect to recognize a positively skewed distribution, with the true burial age situated around the mode of the distribution, and the tail expresses this range of residual ages (left after the last sedimentary cycle). We have to admit, here: the line that separates what was a well-bleached form a partially bleached sediment is blurry, and shrouded in subjectivity. It is possible, but my expert opinion, for the moment, recommends the use of the average. After all, scatter is not that much greater than the notional 20 %, and the average age is 5.8 and 5.9 ka, for both samples. This would be a remarkable coincidence if both samples had been partially bleached. For the sake of completeness, if we assume these were partially bleached, their best age would be younger, at about 4 ka, by using the minimum age model (Galbraith et al., 1999).

Also, the presence of 137Cs, in both samples, is highly problematic. I personally processed these samples. At that time, the lab held no such, very young, 137Cs bearing, samples. The last such sample was processed in early 2020. Since then, we received 3 more such very young samples, but these are still in their tubes, unprocessed.

While we may never exclude contamination during the sample processing, it would be very unlikely, to explain the difference between 100 – 500 ka expectation and the OSL age of 5.8 – 5.9 ka. Even less likely, a contamination from 137Cs. During each and every gamma spectrometry measurements, we always monitor the energy region associated with 137Cs (661 keV). We always record background (i.e. no peak). None should be present, either. But it is simple to monitor the energy region.

Subject subsamples were retrieved, inside the OSL tube, and the gamma spectrum was measured: no 137Cs. Most likely, the 137Cs that was originally detected is limited to the < outside > portion of the OSL tube (about 1 inch of sediment is remove, from both < in > and < out >, mixed together, then its gamma spectrum is measured). It is possible that the surface of the trench was covered by

a modern layer of sediment. That, not enough was removed before inserting the OSL tube. Fortunately, 137Cs was not detected further inside the OSL tubes. Since the IRSL age for both samples is very close, 5.8 and 5.9 ka, it seems plausible that this is the true age of this sedimentary unit. And that, further below, one might find the 100 – 500 ka unit.

5. Uncertainty budget

The breakdown of the uncertainties, between the total random and systematic sources, are presented in table 7. The random uncertainties reflect the standard error on the best estimate (i.e. from the central age model) for the equivalent dose (in seconds of laboratory-induced irradiation). The systematic uncertainties reflect here the combined (in quadrature) components of the environmental dose rate and calibration of the beta source on the luminescence system.

Table 7. Random and systematic uncertainties (in years), at 1 sigma

ISGS code	Sample	Age (ka)	1s (random)	1s (systematic)
953	Ess167	2.968 ± 0.229	± 0.190	± 0.128
954	Ess224	5.804 ± 0.781	± 0.730	± 0.278
955	Ess225	5.939 ± 0.593	± 0.513	± 0.297

6. Conclusion

In summary, the luminescence properties of these K-feldspar minerals behaved reasonably well, as we routinely expect from these minerals. Anomalous fading was measured and corrected with a single aliquot approach. 137Cs was positively detected, in 2 samples, implying a very young, modern, sediment. Fortunately, this was limited to the external portions of the OSL tube. The K-feldspar minerals are always extracted from further inside the tube. The samples appear to have been well-bleached at deposition.

Sebastien Huot, PhD

Illinois State Geological Survey

References

Aitken, M.J., 1998. An introduction to optical dating. Oxford University Press, Oxford.
Auclair, M., Lamothe, M., Huot, S., 2003. Measurement of anomalous fading for feldspar IRSL using SAR. Radiation Measurements 37, 487-492.
Autzen, M., Andersen, C.E., Bailey, M., Murray, A.S., 2022. Calibration quartz: An update on dose calculations for luminescence dating. Radiation Measurements 157, 106828.
Brooks, C., Hart, S.R., Wendt, I., 1972. Realistic use of two-error regression treatments as applied to rubidium-strontium data. Reviews of Geophysics 10, 551-577.
Buylaert, J.-P., Jain, M., Murray, A.S., Thomsen, K.J., Thiel, C., Sohbati, R., 2012. A robust feldspar luminescence dating method for Middle and Late Pleistocene sediments. Boreas 41, 435-451.
Galbraith, R.F., Roberts, R.G., Laslett, G.M., Yoshida, H., Olley, J.M., 1999. Optical dating of single and multiple grains of quartz from Jinmium rock shelter, northern Australia: part I, experimental design and statistical models. Archaeometry 41, 339-364.
Gilmore, G.R., 2008. Practical gamma-ray spectrometry, 2nd ed. John Wiley & Sons, Ltd.
Huntley, D.J., Baril, M.R., 1997. The K content of the K-feldspars being measured in optical dating or in thermoluminescence dating. Ancient TL 15, 11-13.
Huntley, D.J., Hancock, R.G.V., 2001. The Rb contents of the K-feldspar grains being measured in optical dating. Ancient TL 19, 43-46.
Huntley, D.J., Lamothe, M., 2001. Ubiquity of anomalous fading in K-feldspars and the measurement and correction for it in optical dating. Canadian Journal of Earth Sciences 38, 1093-1106.
Huot, S., Lamothe, M., 2003. Variability of infrared stimulated luminescence properties from fractured feldspar grains. Radiation Measurements 37, 499-503.
Ludwig, K.R., 2003. Mathematical-statistical treatment of data nd errors for Th-230/U geochronology, in: Bourdon, B., Henderson, G.M., Lundstrom, C.C., Turner, S.P. (Eds.), Uranium-Series Geochemistry. Mineralogical Society of America, pp. 631-656.
Mahan, S.A., Rittenour, T.M., Nelson, M.S., Ataee, N., Brown, N., DeWitt, R., Durcan, J., Evans, M., Feathers, J., Frouin, M., Guérin, G., Heydari, M., Huot, S., Jain, M., Keen-Zebert, A., Li, B., López, G.I., Neudorf, C., Porat, N., Rodrigues, K., Sawakuchi, A.O., Spencer, J.Q.G., Thomsen, K., 2023. Guide for interpreting and reporting luminescence dating results. GSA Bulletin 135, 1480-1502.
Murray, A.S., Wintle, A.G., 2000. Luminescence dating of quartz using an improved single-aliquot regenerative-dose protocol. Radiation Measurements 32, 57-73.
Wintle, A.G., 1973. Anomalous fading of thermoluminescence in mineral samples. Nature 245, 143-144.